

## FABRIC MAP FOR KAOLINITE: EFFECTS OF pH AND IONIC CONCENTRATION ON BEHAVIOR

ANGELICA M. PALOMINO AND J. CARLOS SANTAMARINA\*

School of Civil and Environmental Engineering, Georgia Institute of Technology, 790 Atlantic Drive, Atlanta, Georgia 30332-0355, USA

**Abstract**—The behavior of fine-grained mineral systems is dependent on pore-fluid characteristics. The systematic analysis of previously published studies supports the development of a fabric map in the pH and ionic concentration space as a working hypothesis. This conceptual study is complemented with an extensive battery of tests where surface charge and particle interactions are controlled through pore-fluid characteristics. The macro-scale tests include sedimentation, viscosity and liquid limit, and involve a wide range of solid volume fractions (suspension to sediment) and strain levels. Experimental results permit the development of an updated fabric map on the pH-ionic concentration space which takes into consideration all experimental results. The fabric map is structured around a critical pH level and a threshold ionic concentration beyond which van der Waals attraction prevails.

**Key Words**—Clay, Double Layer, Electrical Forces, Liquid Limit, Particle-particle Interactions, Sedimentation, Viscosity.

### INTRODUCTION

Particle-to-particle interactions in fine-grained soils are affected by the characteristics of the pore-fluid. This is readily confirmed by analyzing data reported in the classical literature, *e.g.* van Olphen (1977, p. 23), Lambe and Whitman (1969, p. 58), and Mitchell (1993, p. 152). However, trends are not obvious, and often appear to contradict explanations based on simply attraction and repulsion forces between parallel platy particles.

Clay-fabric formation depends primarily on particle size and shape, clay mineralogy and pore-fluid chemistry. These parameters determine the nature of the dominant forces acting on the particles. Previous researchers have studied clay systems over a range of pH, ionic concentration, or both (Sridharan and Prakash, 1999; Melton and Rand, 1977; Fam and Dusseault, 1998; Chen and Anandarajah, 1998; Anandarajah, 1997; Ravisangar, 2001; Pierre *et al.*, 1995; Pierre and Ma, 1999). The purpose of this study is to explore systematically the effect of pore-fluid pH and ionic concentration on macro-scale clay behavior at low effective confinement.

The manuscript starts with a brief review of electrical phenomena affecting fabric formation. A hypothetical kaolinite fabric map describing particle associations with respect to pore-fluid pH and ionic concentration is proposed based on the governing electrical forces and published data. Then, the fabric map is experimentally verified by altering the pore-fluid chemistry as well as concentration of solids through a selected set of simple yet robust and informative laboratory tests.

\* E-mail address of corresponding author:  
carlos.santamarina@ce.gatech.edu  
DOI: 10.1346/CCMN.2005.0530302

### FABRIC FORMATION

Clay fabric is the physical manifestation of the interplay between the various electrical forces and physical phenomena involved in fine-grained minerals. Variables include particle size, mineralogy, structural charge, fluid interactions and electrical double-layer formation, pH and ionic concentration, particle geometry and particle-particle interactions. The effects of each parameter are summarized in Table 1, and a brief discussion follows (for a detailed analysis see Santamarina *et al.*, 2002).

#### *Particle size and shape*

Due to their small size and large specific surface area, clay behavior under low confinement is dominated by interparticle electrical forces rather than by particle self weight. The specific surface may be defined as the ratio of the particle surface area to its mass. The specific surface area,  $S_a$ , of an ideal hexagonal kaolin particle of size  $d$  and thickness  $t$  is:

$$S_a = \frac{8}{\sqrt{3}dp} + \frac{2}{tp} \text{ (hexagonal plate - kaolin)} \quad (1)$$

where the first term is the contribution from the edge and the second term from the faces. Equation 1 shows the significant influence of particle thickness on the specific surface.

#### *Mineralogy*

Mineralogy determines the number and type of reactive sites along the clay particle faces and edges. As shown in Figure 1, kaolinite, a 1:1 clay mineral, consists of a silica sheet and a gibbsite sheet with silicon tetrahedra and aluminum octahedra as the basic units,

Table 1. Phenomena affecting fabric formation summarized from Santamarina *et al.* (2002).

Parameter	Effects on fabric formation
Particle size	Electrical forces control behavior of fine particles ( $d \approx 1-10 \mu\text{m}$ ) at low effective stresses
Mineralogy	Silica and gibbsite stacking of kaolinite, a 1:1 mineral, leaves: $\text{O}^{2-}$ termination sites on the silica face $\text{OH}^-$ termination sites on the gibbsite face $\text{O}^{2-}$ and $\text{OH}^-$ termination sites along the edges (Figure 1d)
Structural charge	General sources: isomorphic substitution broken bonds along termination sites structural disorder and crystal defects Important sources for kaolinite: locally unsatisfied bonds along edges cation ( $\text{Na}^+$ or $\text{Ca}^{2+}$ ) replacement of structural hydrogens on the exposed octahedral basal plane
Fluid interactions and electrical double-layer formation	Dry conditions: structural charges compensated with closely bound counterions excess ions form salt precipitates Wet conditions: precipitated salts hydrate forming bulk fluid electrolyte diffuse double layer – characteristic counterion concentration distribution; thickness, or Debye-Hückel length $\vartheta^*$
	$\vartheta = \left( \frac{\epsilon' k T}{2 c_0 e_0^2 z^2 N_{av}} \right)^{1/2} = \left( \frac{\epsilon' R T}{2 c_0 z^2 F^2} \right)^{1/2}$
pH and ionic concentration	Protonation and deprotonation important at gibbsite face and edge $\text{OH}^-$ termination sites: $M\text{-OH}_{(s)} + \text{H}_{(aq)}^+ \rightleftharpoons M\text{-OH}_2^+$ $M\text{-OH}_{(s)} + \text{OH}_{(aq)}^- \rightleftharpoons M\text{-O}^- + \text{H}_2\text{O}_{(l)}$ Cation adsorption alters charge of $\text{O}^{2-}$ termination sites (silica faces) Differences in basal and edge termination sites lead to independent basal and edge isoelectric points Dissolution reactions and rates are pH dependent
Particle geometry	Impact of double layer increases with decreasing particle size and thickness $t$ Edge potential may be hidden by face double layer for thin particles $t < \vartheta$
Particle-particle interactions	Minimum energy particle associations: EF, EE, FF, shifted FF Interparticle forces that promote these associations include: Coulombian attraction between + edge and face, EF. Osmotic repulsion and van der Waals attraction between two surfaces with like charge. When van der Waals prevails, FF. Prevailing van der Waals attraction at intermediate concentrations, EE. Density and mechanical properties reflect interparticle associations

\*  $T$  – absolute temperature (K),  $c_0$  – bulk solution ionic concentration ( $\text{mol}/\text{m}^3$ ),  $\epsilon'$  – solution real permittivity (farad/m),  $z$  – valence of prevailing cation. Constants: elementary charge ( $e_0 = 1.602 \times 10^{-19}$  C), Boltzmann's constant ( $k = 1.38 \times 10^{-23}$  J/K), Avogadro's number ( $N_{av} = 6.022 \times 10^{23}$   $\text{mol}^{-1}$ ), gas constant ( $R = 8.3145$  J/mol K), and Faraday's constant ( $F = 96485.3$  C/mol).

respectively. Note the differences between boundary groups on the two faces (one  $\text{OH}^-$ , the other  $\text{O}^{2-}$ ) and the presence of both groups on edges.

#### Structural charge

Particle excess structural charges become points of interaction between the mineral surface and ions in the surrounding environment. When dry, structural charges

are compensated with counterions closely bound to the mineral surface. Upon wetting, the counterions hydrate and form the counterion cloud. The counterion cloud thickness or Debye-Hückel length,  $\vartheta$ , depends on the properties of the surrounding fluid (real permittivity, ionic concentration, counterion valence, Lyklema, 1995; Mitchell, 1993). Two important geometric relationships between particles and their respective counterion clouds

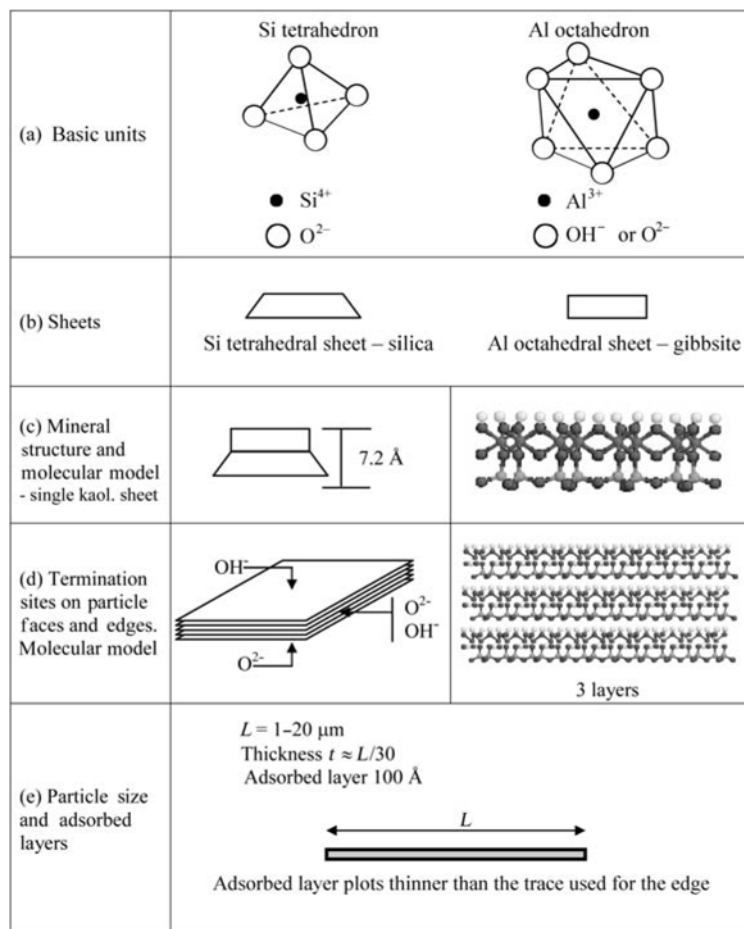


Figure 1. Kaolinite. The primary building blocks (a) and (b), structure (c) edge and face termination sites (d), and particle size and adsorbed layers (e). The molecular model images were prepared using the MDL Chime<sup>®</sup> web browser plug-in (Barak and Nater, 2003).

must be considered: (1) the impact of the counterion cloud increases with decreasing particle size and thickness; and (2) the edge potential may be hidden by the face counterion cloud when particles are thin  $t < \lambda$  (Secor and Radke, 1985).

#### Influence of pH

Mineral stability depends on the surrounding fluid pH, ionic concentration, ion type, and temperature, and the particle can be rendered negatively or positively charged. Mineral-surface charge modification occurs through the processes of protonation, deprotonation and cation complexation (Stumm, 1992). The pH dependence of kaolinite dissolution involves two distinct mechanisms: (1) at low pH, Al dissociates preferentially (Wieland and Stumm, 1992); and (2) at high pH, silica dissociates preferentially (Brady and Walther, 1989). Differences in termination sites on clay-particle basal surfaces and edges may lead to each surface having its own corresponding isoelectric point (IEP). Mineral

dissolution shifts the pH towards a stable value corresponding to the particular mineral-fluid system by consuming H<sup>+</sup> at low pH and OH<sup>-</sup> at high pH (Santamarina *et al.*, 2002).

#### Influence of ionic concentration

The double layer or osmotic repulsion between two parallel circular disks separated by a distance  $x$  can be estimated as (Israelachvili, 1992)

$$F_{DL} = 16\pi R T c_o d^2 e^{-x/\lambda} \quad (2)$$

where  $c_o$  is the bulk fluid ionic concentration,  $R$  the gas constant, 8.314 J/(mol K), and  $T$  the absolute temperature. On the other hand, the van der Waals attraction force is (Israelachvili, 1992)

$$F_{Att} = \frac{1}{24} \frac{A_h}{x^3} d^2 \quad (3)$$

where  $A_h$  is the Hamaker constant. Note that the Hamaker constant is not sensitive to the ionic concen-

tration; therefore,  $F_{Att}$  remains relatively constant as  $c_o$  increases. However,  $F_{DL}$  decreases. Hence, it is anticipated that there is a threshold concentration,  $c_{th}$ , that, once exceeded, causes the two platy particles to approach each other spontaneously.

#### Particle associations

Governing interparticle forces determine the association between two particles. These associations may be classified as edge-to-face (EF), edge-to-edge (EE), or face-to-face (FF) (van Olphen, 1977). A fourth association often observed in scanning electron microscopy (SEM) images is shifted face-to-face (shifted FF). Interparticle forces that promote these associations include: Coulombian attraction between a positive edge and a negative face (EF – Schofield and Samson, 1954); osmotic repulsion and van der Waals attraction between two like-charged surfaces (FF occurs when van der Waals attraction prevails, otherwise the systems remain dispersed); and prevailing van der Waals attraction between edges while interfacial interaction remains repulsive (EE). The density and mechanical properties of the sediment will reflect the type of interparticle associations. For example, FF aggregations typically form high-density flocs, and EF flocs experience strong Coulombian and van der Waals attraction forces.

Note that these particle-to-particle associations group to form larger aggregates, linking through EE and EF interactions and form high void-ratio networks (van Olphen, 1977; Rand and Melton, 1977; Melton and Rand, 1977; O'Brien, 1971).

#### Postulated kaolinite fabric map

The previous discussion suggests that particle associations are a function of pH (surface charge control) and ionic concentration (balance between  $F_{DL}$  and  $A_{it}$ ). Thus, the fabric map in Figure 2 can be constructed to summarize particle interactions for kaolinite across a range of pH values and ionic concentrations. This fabric

map is based on published data found in the literature (Schofield and Samson, 1954; O'Brien, 1971; van Olphen, 1977; Rand and Melton, 1977; Melton and Rand, 1977). The prevailing considerations for each region in the proposed 'pH-concentration fabric map' follow:

**Low ionic concentration region ( $c_o < c_{th}$ ).** In the low-ionic concentration region, the kaolinite suspension behavior is pH dependent. At high pH, both the particle edges and faces are negatively charged, the double layer is large, and repulsion prevails. The particles are therefore deflocculated and dispersed. As the pH decreases and becomes less than the edge IEP (pH  $\approx$  7.2), the particle net positive edge charge increases due to protonation and electrostatic attraction favors EF associations. When the pH approaches the particle (face) IEP, there is no global repulsion. Van der Waals-dominated associations are expected. Finally, at low pH, both the particle edges and faces are positively charged (at least the gibbsite faces, while the silica faces have minimal net charge; Brady and Walther, 1989). This results in deflocculated-dispersed structure.

Mineral dissolution and release of  $Al^{3+}$  ions at extremely low pH (<2) and silica dissolution at high pH (>9) are expected to induce particle coagulation. Release of  $Al^{3+}$  and subsequent surface re-adsorption induces rapid particle coagulation in FF aggregates (Rand *et al.*, 1980; Wieland and Stumm, 1992).

**High ionic concentration ( $c_o > c_{th}$ ).** At NaCl electrolyte concentrations >0.1–0.15 mol/L, the double layer is thin, van der Waals attraction dominates, and particles associate in FF aggregation. Shifted FF may be observed in the pH region below the edge IEP and above the face IEP.

**Moderate ionic concentration.** As the ionic concentration increases from low to high, particle associations shift from deflocculated-dispersed or EF to FF aggregation. In the transition region ( $\sim$ 0.1 mol/L NaCl), the

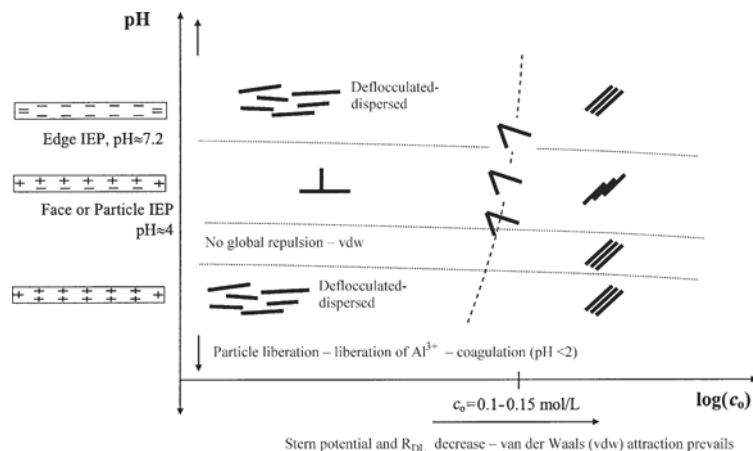


Figure 2. Hypothesized fabric map (after Santamarina *et al.*, 2002). Summary of postulated particle associations (preferred minimum energy configurations) for kaolinite in NaCl electrolytes. Synthesis based on published data.

expected particle association is EE and is independent of pH (at moderate pH values).

### EXPERIMENTAL METHODOLOGY

Particle interactions were determined by assessing the state of dispersion of clay specimens mixed with pH-modified electrolytes. Three different test series were performed to study the effects of pH and ionic concentration on clay fabric: sedimentation tests, rheological/viscosity tests, and liquid limit measurements. A brief description of material preparation, test procedures and their interpretation follows.

#### Materials

This study focuses on the behavior of a single type of kaolin, Wilklay RP2. The kaolin is an air-float processed clay, with a specific gravity  $G_s = 2.6$  and an average diameter  $d_{50} = 0.36 \mu\text{m}$  (Wilkinson Kaolin Associates, Georgia). This clay was selected because no chemicals are added during processing. A SEM image of this clay, as received, is shown in Figure 3.

The kaolin was rendered monoionic using procedures similar to those outlined by van Olphen (1977). The clay was mixed vigorously with a 2 mol/L NaCl solution at  $\sim 3$  mL of solution per gram of kaolinite. The suspension was left for 48 h, during which the clay particles were allowed to settle. The supernatant liquid was siphoned and replaced with a 1 mol/L NaCl solution, mixed and left for 24 h. The process was repeated with another 1 mol/L NaCl solution wash for a total equilibrium time of 96 h. After the final salt wash, the excess salt was removed through several washings with deionized water (typically 10 or more). The supernatant liquid conduc-

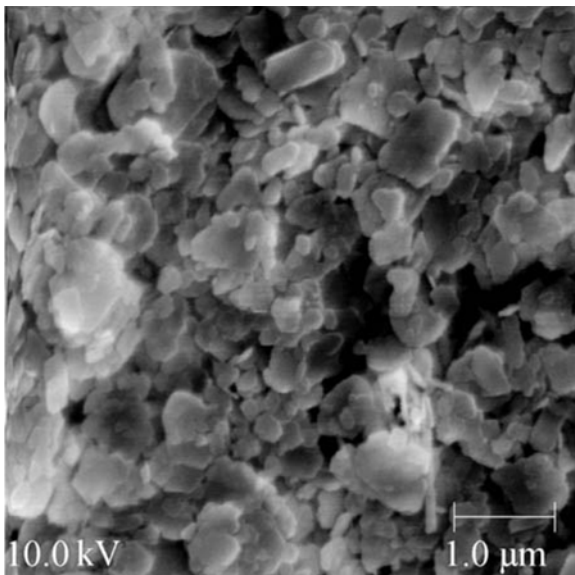


Figure 3. SEM image of untreated RP2 kaolinite.

tivity was measured periodically with an Omega Conductivity Meter (model CDB 420). The clay was considered 'monoionic with no excess salts' when the supernatant liquid conductivity was  $<100 \mu\text{S/cm}$ . The clay was then oven dried and ground into powder form using a pestle and mortar.

Specimens for all tests were prepared with NaCl solutions at concentrations of  $10^{-5}$ ,  $4 \times 10^{-4}$ ,  $3 \times 10^{-3}$ , 0.1 and 1.8 mol/L. The target pH values for the solutions were 3, 5, 7 and 9 at each concentration for a total of 20 solutions. The pH was altered with  $\text{HNO}_3$  to lower the pH, and NaOH to raise it.

#### Test procedures and physical interpretation

**Sedimentation.** The state of dispersion of a suspension with a low solids content may be inferred from the settlement behavior just after mixing as well as the final sediment volume. Previous authors have defined the various sedimentation modes that are typically observed (Patton, 1979; Imai, 1980; Ravisangar, 2001; Pierre and Ma, 1999). It is important to note that these authors made no distinction between EF flocculation or FF aggregation within the flocculation sedimentation behavior classification. However, Pierre *et al.* (1995) verified the structures for kaolinite sediments formed from suspensions exhibiting flocculation and dispersed settling behaviors using SEM. For this study, sedimentation behavior was categorized as EF flocculated, FF aggregated, dispersed, or mixed-mode as defined in Table 2. Also, particle associations are defined as flocculated for EF associations, aggregated for FF associations and dispersed for particles with minimal interaction. Criteria outlined in Table 2 combine the experience documented by previous researchers and gathered in this study.

Suspensions for sedimentation tests were prepared so that the solids volume fraction was  $\phi = 0.02$  ( $\phi$  is the total volume of solids divided by the total suspension volume). A 2.54 cm diameter acrylic cylinder was filled with  $\sim 10$ – $20$  mL of the selected pore-fluid solution. The oven-dried and ground clay (3.93 g) was mixed gently with the fluid in the cylinder; then more pore-fluid added to the cylinder to reach a total height of 15.5 cm, corresponding to 78.5 mL. The suspension was mixed slowly with a perforated plunger until a uniform appearance was observed. The suspension hydrated overnight and was then remixed.

Entrapped air is removed with a low vacuum (vacuum pressure  $u \cong -5$  kPa). After the air had evacuated (no evidence of bubble formation), the cylinder was repeatedly inverted for  $\sim 1$  min without releasing the vacuum.

After the last inversion, the cylinder was placed on a level surface. This instant is considered time zero. The vacuum was removed, and the cylinder was capped with a rubber stopper. Both the suspension and sediment heights were monitored with time. The heights were recorded starting at  $t = 15$  s. Each subsequent reading

Table 2. Suspension settlement modes defined for this study.

Sedimentation characteristics	Mode			
	Dispersed sedimentation	EF flocculation sedimentation	FF aggregation sedimentation	Mixed-mode sedimentation
Particle interaction	Minimal; any aggregates formed remain dispersed	Strong; flocs form readily	Strong; aggregates form readily	Minimal → floc/agg. formation
Suspension appearance	Milky with increasing density from top to bottom	Uniform density	Uniform density	Top to bottom increasing density → uniform
Supernatant liquid appearance	Cloud of suspended fine particles	Clear	Clear	Cloudy → Clear
Suspension-supernatant liquid interface	None	Well defined, moves downwards as flocs settle	Well defined, moves downwards as aggregates settle	None → well defined
Suspension-sediment interface	Well defined, moves upwards as sediment builds	None	None	Well defined → none
Settlement rate	Very slow	Rapid, constant	Very rapid, constant	Slow → rapid
Sediment formation	Particles settle into lowest possible position and according to size, largest first	Flocs settle in random pile	Aggregates settle according to size	Particles settle according to size → Formed flocs/aggregates settle uniformly
Sediment volume	Compact; strongly resists redispersion	Voluminous; easily redispersed	Compact to voluminous	Layer of compact sediment below layer of voluminous sediment

was taken at twice the time interval of the previous reading, *i.e.*  $t_1 = 15$  s,  $t_2 = 30$  s,  $t_3 = 1$  min, *etc.* Suspension and sediment heights were recorded for 2 weeks. Then, the supernatant liquid pH of each suspension was measured using an Accumet AR50 pH meter (Fisher Scientific). Adjustments to pH were made by adding small volumes of extreme pH solutions prepared at the appropriate salt concentration. The suspensions were remixed and measurements recorded according to the selected time schedule for 91 days. The supernatant liquid pH was measured again at the end of 91 days.

*Viscosity.* Well dispersed kaolinite suspensions at low solids content have been shown to yield a much lower viscosity than that of a flocculated system with an equal solids content (Rand & Melton, 1977; Nicol & Hunter, 1970; Michaels & Bolger, 1964). Low viscosity is due to particle or flow-unit alignment so that the platy particles have a minimal contribution to flow resistance. Deflocculation results in a decrease in viscosity.

Decreasing viscosity with increasing shear rate characterizes shear thinning or pseudoplastic fluid. If this effect depends on the shear history of the fluid, the behavior is termed thixotropic and is a typical characteristic of flocculated clay suspensions (Hiemenz, 1986; van Olphen, 1977). Clay suspensions typically exhibit either shear thinning or near-Newtonian behavior. Shear thinning behavior is associated with defloc-

ulation in that the number of interparticle bonds in a flocculated suspension decreases with increasing shear rate (Hunter, 2001). In other words, increasing the applied stress breaks down the suspension structure into smaller flow units the size and particle associations of which depend on the interparticle forces (Rand & Melton, 1977).

Suspensions for viscosity tests were prepared with a solids volume fraction of  $\phi = 0.07$  in a 600 mL beaker. The clay was mixed with the selected pore-fluid solution to form a 400 mL suspension. The beaker was placed on a Corning magnetic stirrer and mixed for 8 h prior to measurement. After the equilibration time, the pore-fluid pH was verified and corrected as needed.

The suspension viscosities were measured using a Brookfield DV-E Viscometer fitted with Spindle #1 ( $d = 56.26$  mm). The spindle rotational speed was varied between 1 rpm and 100 rpm, and the viscosity reading and degree of settlement recorded after 1.5 min for every rotational speed setting. Between readings, the suspensions were mixed well for ~20 s to re-mix particles that may have settled. The final pore-fluid pH was determined by centrifuging a small sample and measuring the supernatant liquid.

*Liquid limit.* The liquid limit is the water content boundary dividing the plastic and liquid behavioral states of a clay. Soils at the liquid limit have a shear strength between 1.3 and 2.4 kPa (Wroth and Wood,

1978). The shear strength of a clay at its liquid limit depends on the clay fabric, as particles or aggregates interact to supply the resistance to shear (Mitchell, 1993).

The British fall-cone test standard (British Standard 1377, 1990) defines the liquid limit as the water content at which an 80 g stainless steel cone with a 30° angle penetrates a remolded soil 20 mm specimen when the cone is released at the soil surface. Penetration measurements were taken with a Wykeham Farrance cone penetrometer at three moisture contents for each remolded mineral mixture. The first moisture content was obtained by mixing ~50–100 mL of electrolyte solution with 200–350 g of solids. Typical solid-liquid volume fractions for kaolinite near the liquid limit were  $\phi = 0.50$  to 0.85 (the exact solution volumes were recorded). The clay mixture hydrates for at least 8 h before obtaining the first measurement point. After the equilibration time, the clay was thoroughly re-mixed and carefully placed in a metal cup, 6.25 × 4.5 cm, avoiding air entrapment. The excess material was scraped off the top leaving a smooth even surface. Once an acceptable penetration depth was recorded, 10 to 30 g of material were removed to determine the moisture content. The pore-fluid pH was measured by placing a small amount of the mineral paste on the reactive portion of a ColorpHast pH strip (Fisher Scientific) and allowing the pore-fluid to leach onto the paper. The remaining clay was then mixed with additional fluid volume to

increase the moisture content for the next penetration measurement. Cone penetration depths were plotted against percentage moisture contents. Reading from a best-fit line drawn through the measured points, the moisture content corresponding to 20 mm penetration was determined. The sensitivity to pore-fluid content was denoted by the slope of the measured cone penetration vs. water content at the liquid limit. The greater the slope, the more rapidly the clay shear strength reduces for a given increase in water content.

## EXPERIMENTAL RESULTS

Table 3 summarizes the results obtained for all sedimentation, viscosity and liquid limit tests. A detailed analysis of each set of results follows.

### *Sedimentation behavior*

Sedimentation trends are plotted in Figure 4. The observed sedimentation behavior for the tested kaolinite suspensions is summarized in Table 3 (observed suspension modes are categorized according to the definitions presented in Table 2). Salient observations include:

All suspensions at pH 3 exhibit characteristics consistent with FF aggregation sedimentation independent of ionic concentration.

At pH 5 and high ionic concentration ( $c > 0.1$  mol/L), the suspension settling mode is mixed with a thin colloidal cloud lasting for several hours.

Table 3. Summary of results: sedimentation, viscosity and fall cone test data.

NaCl concentration (mol/L)	Target pH	Sedimentation (0.02 solids content)				Viscosity (0.07 solids content)		Fall cone (0.55–0.85 solids content)		
		Measured pH	Observed mode	$\alpha$ (cm/min)	Final height (cm)	Measured pH	Viscosity (mPa s)	Measured pH	LL slope (mm/w%)	Liquid limit
$10^{-5}$	3	3.03	Flocculation	8.5	1.55	2.91	34.5	5.3	0.457	66.9
	5	4.50	Mixed	2.4	2.35	5.07	68.6	4.7	0.544	69.3
	7	6.53	Dispersed	1.8	2.20	6.81	83.2	4.8	0.486	63.7
	9	8.45	Dispersed	0.2	2.25	8.50	16.5	5.8	0.570	65.0
$4 \times 10^{-4}$	3	3.50	Flocculation	3.5	2.25	3.43	56.8	5.2	0.443	67.3
	5	4.27	Mixed	1.7	2.75	5.35	95.8	4.7	0.519	68.9
	7	6.70	Dispersed	1.1	2.75	6.71	156.8	5.7	0.488	68.0
	9	8.55	Dispersed	1.2	2.95	8.11	18.2	5.7	0.477	65.0
$3 \times 10^{-3}$	3	3.33	Flocculation	3.7	2.45	3.44	49.1	6.0	0.536	66.0
	5	5.23	Mixed	2.0	2.65	5.03	64.4	4.3	0.476	65.3
	7	6.87	Mixed	2.1	2.45	6.51	99.5	6.0	0.455	68.1
	9	8.86	Mixed	1.1	2.95	8.99	15.8	6.0	0.543	66.7
0.1	3	3.39	Flocculation	0.7	2.80	3.10	46.5	5.7	0.755	57.7
	5	4.34	Mixed	0.9	2.70	4.62	49.6	4.3	0.742	57.0
	7	7.14	Mixed	0.8	2.60	6.37	44.8	6.0	0.785	56.8
	9	8.53	Mixed	0.7	2.45	8.67	53.5	5.8	0.780	58.4
1.8	3	3.35	Flocculation	0.05	2.95	3.26	78.8	3.8	0.895	48.2
	5	4.70	Dispersed	0.06	2.25	4.44	69.9	4.0	1.51	51.7
	7	7.23	Dispersed	0.07	2.75	6.72	60.6	3.8	0.677	60.2
	9	8.56	Dispersed	0.04	2.90	8.82	81.4	3.8	0.894	54.8

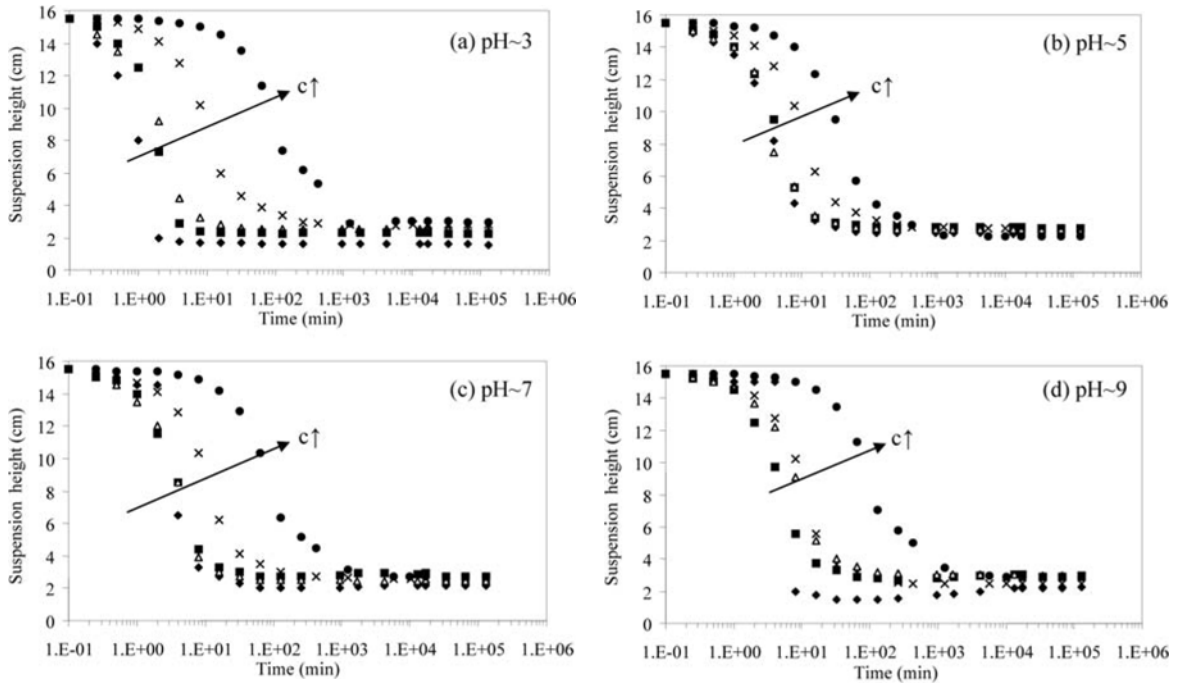


Figure 4. Kaolinite sedimentation curves. Cases are for target pore-fluid pH: (a) 3, (b) 5, (c) 7 and (d) 9. Pore-fluid NaCl concentrations in mol/L:  $\blacklozenge$   $10^{-5}$ ,  $\blacksquare$   $4 \times 10^{-4}$ ,  $\triangle$   $3 \times 10^{-3}$ ,  $\times$  0.1;  $\bullet$  1.8.

At pH 7 and 9 and intermediate salt concentrations ( $c = 3 \times 10^{-3}$  to 0.1 mol/L), suspension settling is characterized as mixed-mode, *i.e.* initially dispersed then EF flocculated settling, while at high salt concentration ( $c = 1.8$  mol/L) the behavior is mixed with complete settling of colloidal particles taking several hours.

The settlement time and number of suspended particles in the colloidal clouds varies from several hours to 1 month, depending on both electrolyte pH and ionic concentration.

The settling velocity,  $\alpha$  (cm/min), is herein defined as the slope of the initial portion of the settlement-time curve known as the induction period. It is calculated from each suspension settlement curve (linear-linear scale). During the induction period, the initial suspension consists of interconnected flow units with highly tortuous fluid flow paths between them, hence initial fluid displacement is hindered. As time progresses, the flow units tend to line up, shortening the flow paths (Michaels and Bolger, 1962). This marks the beginning of hindered settlement. Therefore,  $\alpha$  indicates how long the suspension flow units interact with each other and how ordered the suspension structure becomes. The settling velocity for each suspension is plotted in Figure 5a. There is a general decrease in  $\alpha$  with increasing ionic concentration for  $c > \sim 10^{-2}$  mol/L. The initial settling velocity for the specimen with  $c = 10^{-5}$  mol/L and pH = 9 is very low, in agreement with the observed sedimentation mode.

The final sedimentation height for each suspension is plotted in Figure 5b. Overall, the sedimentation height

tends to increase with increasing ionic concentration, contrary to predictions based on repulsion and van der

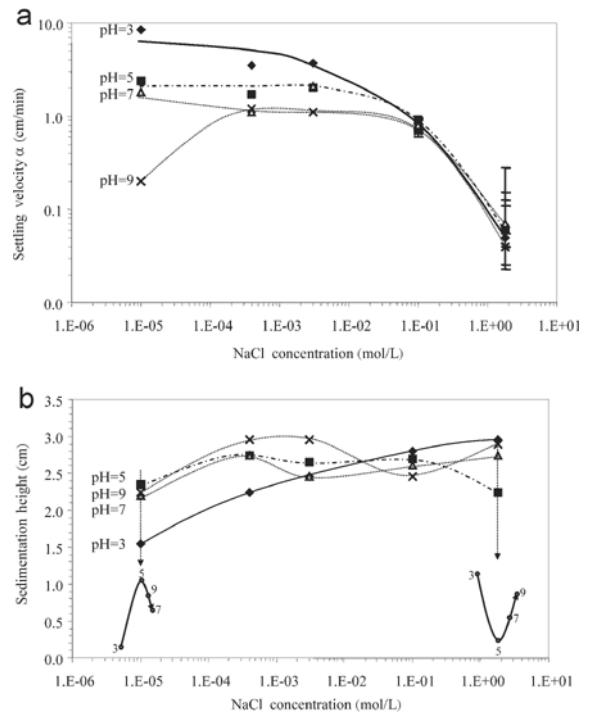


Figure 5. Kaolinite (a) suspension initial settling velocity,  $\alpha$ , and (b) sedimentation height at 91 days. Target electrolyte pH: 3, 5, 7 and 9. Schematic trends shown in (b) highlight the reversal in sedimentation height with pH at extreme NaCl concentrations.



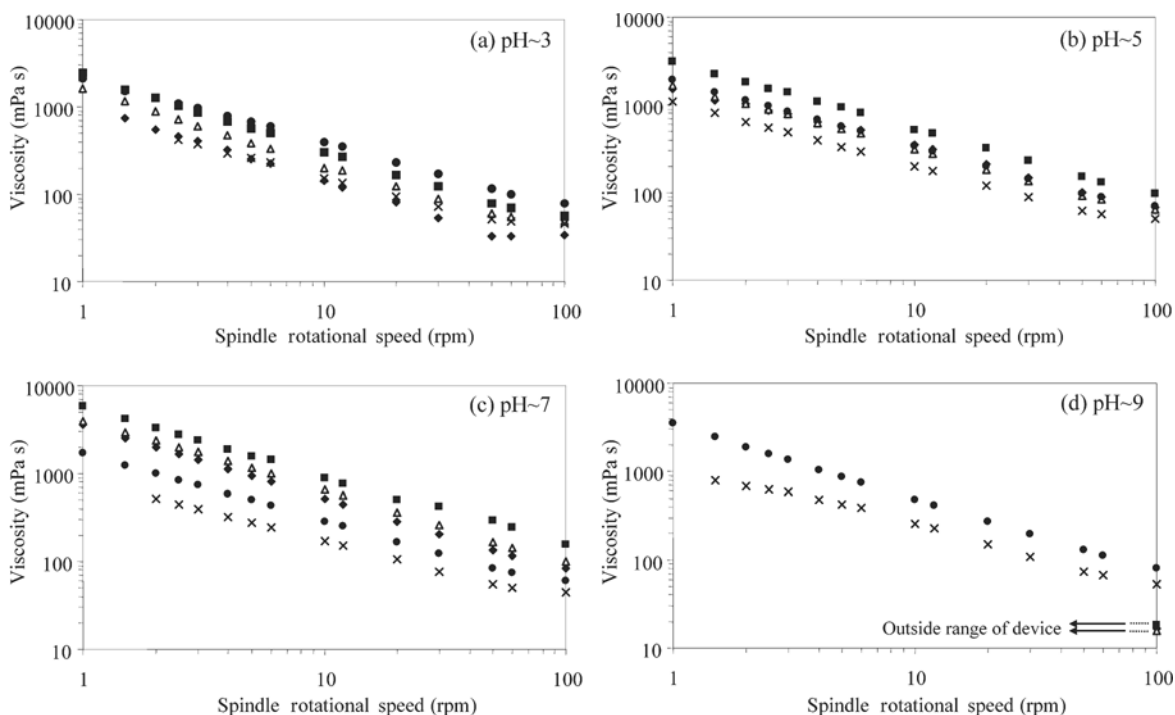


Figure 6. Kaolinite suspension rheological behavior with respect to pH. Cases are for target pore-fluid pH: (a) 3, (b) 5, (c) 7 and (d) 9. Pore-fluid NaCl concentrations in mol/L:  $\blacklozenge$   $10^{-5}$ ;  $\blacksquare$   $4 \times 10^{-4}$ ;  $\blacktriangle$   $3 \times 10^{-3}$ ;  $\times$  0.1;  $\bullet$  1.8.

Waals forces between parallel platelets. This highlights the role of fabric. Notice that there is a reversal on the effect of pH: at low ionic concentration, the sediment height is at a maximum at pH = 5, but it is at a minimum at pH = 5 when the ionic concentration is high. The sedimentation height trends converge at  $\sim 0.02$  mol/L to a single point of  $\sim 2.6$  cm.

*Viscosity*

The general rheological response to increasing shear rate for the suspensions tested in this study is shown in Figure 6. The observed decrease in measured viscosity with increasing shear rate is typical of shear-thinning fluids.

Viscosities at 100 rpm are plotted vs. ionic concentration in Figure 7. Below the ionic concentration of 0.1 mol/L, the viscosities increase with the pH up to pH = 7, indicating the direction of increasing flocculation. At concentration  $c \approx 0.05$  mol/L, the viscosities tend toward a single value ( $\sim 49$  mPa s) regardless of pH. Above concentration  $c \approx 0.05$  mol/L, the effect of pH on viscosity reverses and the lowest viscosity is measured at pH = 7.

*Liquid limit*

Fall cone penetration lines are shown in Figure 8. Liquid limits and penetration vs. water content slopes are summarized in Figure 9a,b. Overall, the liquid limit decreases with increasing salt concentration. The solution pH has the greatest impact on liquid limit at extreme

ionic concentrations. Liquid limit for all pH values converge for  $c \approx 0.02$  mol/L to a single point LL  $\approx 63\%$ .

The sensitivity of penetration depth to water content increases with increasing ionic concentration. Slope values collapse to a single point at  $c \approx 0.08$  mol/L NaCl regardless of solution pH, even though the solution pH has little impact on slope except at very high NaCl concentrations, *i.e.* 1.8 mol/L.

DISCUSSION

This study maps the interactions of clay particles within a wide range of pore-fluid pH (pH = 3 to pH = 9),

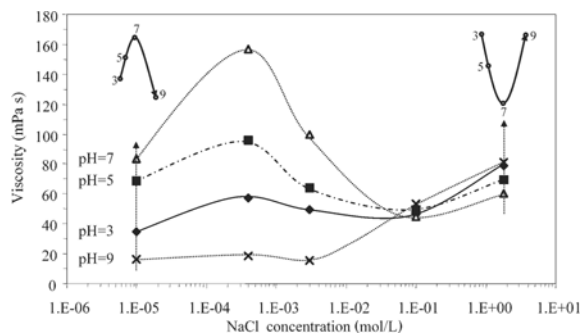


Figure 7. Kaolinite suspension viscosities at 100 rpm using Spindle #1. Schematic trends highlight the reversal in viscosity with pH at extreme NaCl concentrations.

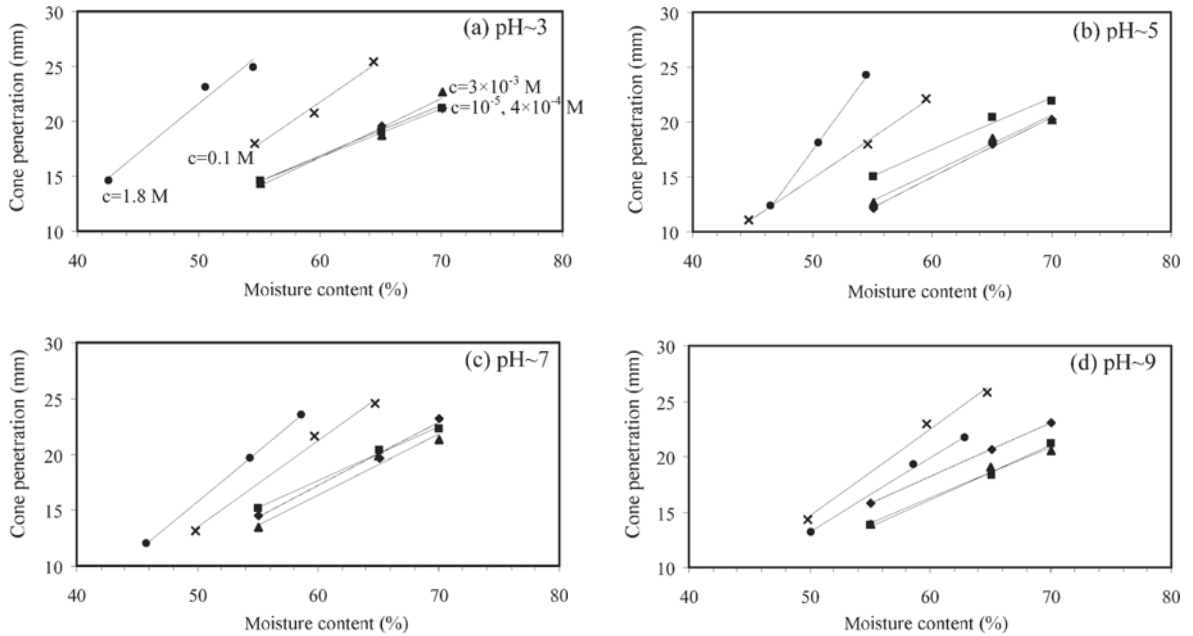


Figure 8. Kaolinite fall cone penetration lines. Cases are for target pore-fluid pH: (a) 3, (b) 5, (c) 7 and (d) 9. Pore-fluid NaCl concentrations in mol/L:  $\blacklozenge$   $10^{-5}$ ;  $\blacksquare$   $4 \times 10^{-4}$ ;  $\blacktriangle$   $3 \times 10^{-3}$ ;  $\times$  0.1;  $\bullet$  1.8.

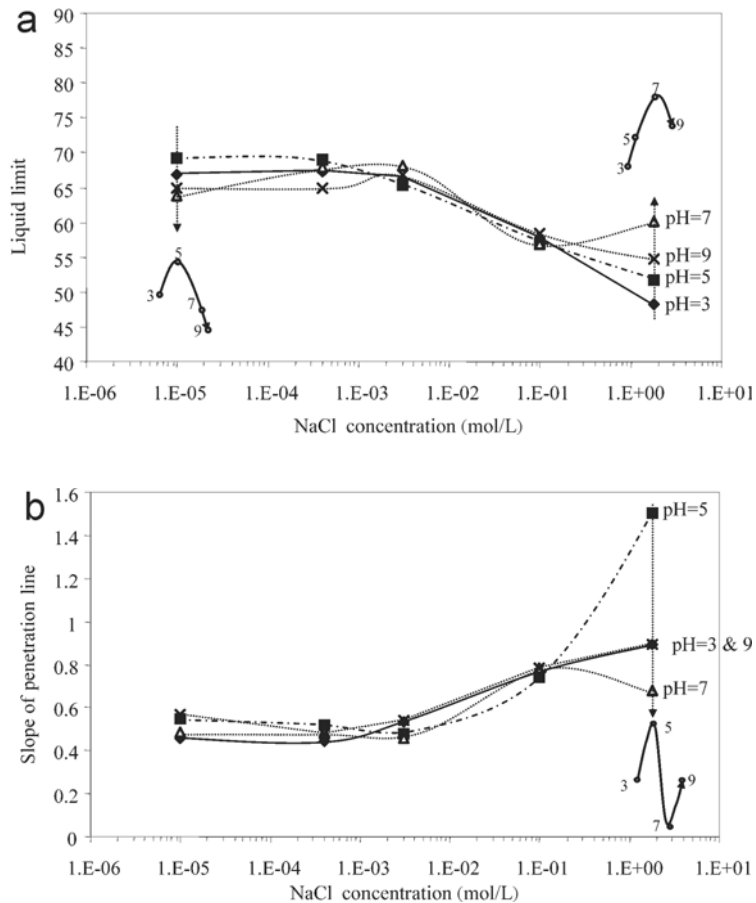


Figure 9. Kaolinite fall cone (a) liquid limit and (b) slope of penetration line. Target electrolyte pH: 3, 5, 7 and 9. Schematic trends are also represented.

ionic concentration ( $c = 10^{-5}$  mol/L to  $c = 1.8$  mol/L), range of solids concentrations ( $\phi = 0.02$  to  $\phi = 0.85$ ) and physical disturbances – either strain level or strain rate.

#### *Low/intermediate solids concentration*

The DLVO theory predicts particle repulsion and a dispersed system at very low ionic concentrations and low valence, in this case  $10^{-5}$  NaCl. However, the sedimentation and rheological behaviors are pH dependent at this concentration. At pH 3, the low final sedimentation height, low viscosity and high initial settling velocity,  $\alpha$ , indicate that the low and moderate solids suspensions are dispersed. But, the settling behavior is observed to have a high degree of particle interaction. In addition, kaolinite particle dissolution is significant at low pH. For this case, dissolution promotes face-to-face aggregation forming dense, yet dispersed, aggregates (verified with SEM). Dispersed FF aggregates have a high settling velocity due to the increased aggregation, form a more compact sediment, and cause fewer perturbations in stream lines compared to open EF flocs.

At low ionic concentration and high pH, the observed settlement behavior, settling velocity,  $\alpha$ , and the measured viscosity indicate a dispersed system, consistent with previous findings (Rand and Melton, 1977; Nicol and Hunter, 1970; Michaels and Bolger, 1964) and visual observation using SEM. However, the sedimentation height is greater than expected for a dispersed system. In part this is due to a change in behavior in the suspension: particles that remain in suspension the longest, forming the colloidal cloud, finally interact and form a loosely flocculated structure on top of the initial denser sediment.

At low ionic concentration and moderate pH, the observed and measured parameters indicate a more flocculated structure than that at the extreme pH. Since the measured pore-fluid pH is between the edge and particle isoelectric points, the most likely association for these suspensions is edge-to-face. Increasing the ionic concentration to  $c = 4 \times 10^{-4}$  and  $c = 3 \times 10^{-3}$  increases particle flocculation as indicated by the sedimentation and rheological parameters. At high pH, these systems are dispersed (while high sedimentation heights are observed).

Approaching 0.1 mol/L NaCl, the suspension structure becomes pH independent. This is consistent with previous findings and is attributed to an increase in face-to-face aggregation from edge-to-face due to double layer thinning and subsequent dominance of van der Waals attractive forces (Schofield and Samson, 1954; Rand and Melton, 1977). At this NaCl concentration, the effects of dissolution only contribute to the aggregation process. The extreme pH suspensions show an increase in aggregation, while the moderate pH suspensions tend towards a slight decrease in flocculation behavior compared to the  $c = 3 \times 10^{-3}$  NaCl suspensions. The

thinner double layers allow edge-to-edge and edge-to-face flocs to form (meso-scale) from the face-to-face aggregates.

At  $c = 1.8$  mol/L NaCl, the relative behaviors of the tested suspensions indicate only a slight dependence on pH. For pH 3, all sedimentation and rheological parameters indicate an increase in aggregation from the  $c = 0.1$  mol/L NaCl case. The observed settling behaviors for the remaining pH suspensions indicate slightly less aggregated systems. However, initial settling velocities, sedimentation heights and viscosities show an increase in aggregation. The initial settling velocity increases with increasing ionic concentration, thus indicating an increase in particle associations with salt concentration. Hence, the FF aggregates tend to form EF meso-scale flocs.

#### *High solids concentration*

The liquid limit results agree with experimental data gathered by previous researchers and are attributed to the decrease in double layer thickness: as the double layers shrink, the clay structure becomes more compact and reduces the amount of pore-fluid necessary to induce particle mobilization (Klein, 1999; Di Maio, 1996). This observation suggests that the high volumetric solids content and high strain conditions promote particle alignment and hinder EF flocculation. Consequently, the liquid limit depends primarily on the thickness of the double layer. (Note that the effect of concentration is the opposite for sedimentation height where fabric controls the final volumetric solids content).

The effect of pH on the liquid limit is insignificant at NaCl concentrations  $\leq 0.1$  mol/L. The high solids content increases the buffering capacity of the system through particle dissolution, thereby neutralizing the pore-fluid pH. Dissolving kaolinite particles consume  $H^+$  at low pH and  $OH^-$  at high pH as discussed previously. Dissolution also increases the pore-fluid ionic strength with the release of  $Al^{3+}$  ions. The measured pore-fluid pH for these mixtures ranges from 4.3 to 6.0 even though the starting solution pH prior to mixing with the solids ranges from 2.9 to 8.8 (Table 3, Figure 10). But, at high ionic concentration, 1.8 mol/L, the measured pore-fluid pH ranges from 3.8 to 4.0 (the initial pH of the corresponding solutions ranges from 2.6 to 8.7). These results suggest that the role of the  $Na^+$  ions takes precedence at this concentration, exchanging with  $H^+$  ions on the clay surface to produce a low-pH pore-fluid (Figure 10). Cation-exchange reactions tend to be both stoichiometric and rapid and so can be seen at this testing timescale (Bohn *et al.*, 1985). Klein (1999) makes similar observations of a decrease in pore-fluid pH from 6.01 to 3.82 corresponding to an increase in ionic concentration from  $1 \times 10^{-5}$  to 1.8 mol/L NaCl in low solids content kaolinite suspensions. The  $Na^+ - H^+$  exchange allows for variation in structure and sensitivity at differing pH.

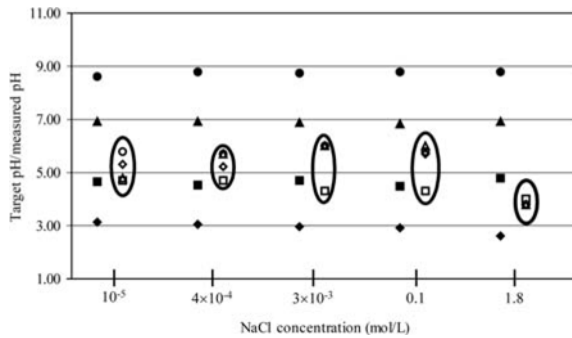


Figure 10. Changes in fluid pH due to particle dissolution during sedimentation. Closed symbols represent electrolyte pH prior to mixing and open symbols represent the measured pore-fluid pH after mixing.

#### Salient trends and relation to previously hypothesized fabric map

Three salient global trends are observed taking into consideration the various results at significantly different solids volume fraction  $\phi$  and strain levels.

The measured clay suspension parameters converge and cross within a range of salt concentrations that varies between 0.02 and 0.1 mol/L NaCl. This is referred to herein as the threshold concentration  $c_{th}$ .

Ionic concentration controls behavior at high concentration, above the transition or threshold concentration  $c_{th}$  ( $c > c_{th}$ ).

Conversely, the effects of pH are greatest at low NaCl concentrations ( $c < c_{th}$ ). In particular, a prominent feature is the impact of EF aggregation on viscosity near the edge and face isoelectric points.

A modified fabric map based on the sedimentation and rheological parameters for the RP2 kaolinite gathered in this research is shown in Figure 11. This map and observed trends are in general agreement with the major characteristics of the proposed fabric map for

kaolinite and NaCl presented in Figure 2 which was derived from conceptual considerations and a synthesis of published results obtained by various authors using different sources of kaolinite.

## CONCLUSIONS

Fabric formation in kaolinite mixtures governs the settlement and rheological behaviors as well as the measured shear strength. Sedimentation, viscosity and fall-cone tests involve widely differing solids volume fraction values,  $\phi$ , and strain conditions. Together, they permit us to infer clay-particle interactions and resulting fabric. For the tested kaolinite clay:

pH has the greatest influence at low pore-fluid salt concentrations. At the highest tested ionic concentration, the sodium-hydrogen exchange results in a low pore-fluid pH as well as an increase in variation of both the liquid limit and the clay sensitivity at varying initial solution pH

There exists a 'convergence ionic concentration' at which the mixture behavior is pH independent. This concentration represents the transition zone between 'primarily' pH-controlled fabric and 'primarily' concentration-controlled fabric.

For high solids-concentration mixtures, the clay buffering capacity neutralizes the solution pH. The liquid limit is thereby only dependent on the ionic concentration. Furthermore, high solids-volume fraction,  $\phi$ , and high strain hinder natural trends in fabric formation and encourage particle alignment.

Therefore, while the role of fabric is highlighted in sedimentation tests (where the sedimentation height increases with concentration), the effect of double layer thickness in aligned particles is magnified in liquid-limit tests (where the liquid limit decreases with increasing ionic concentration).

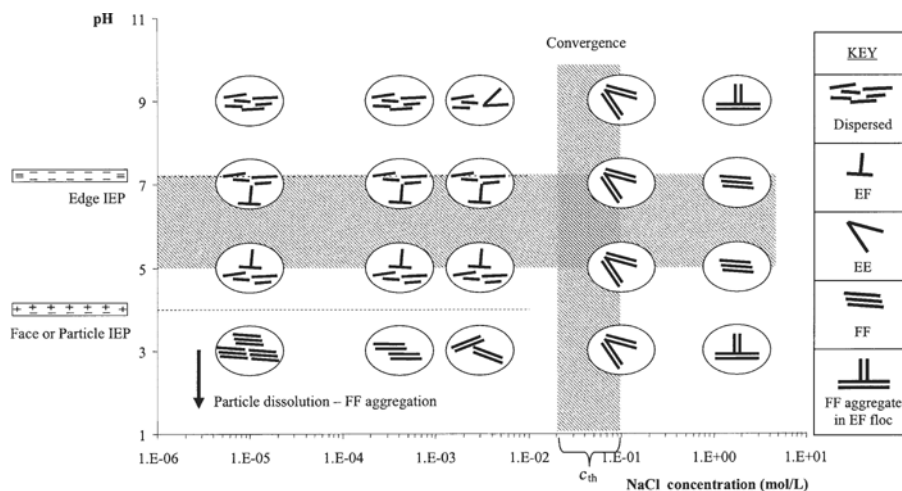


Figure 11. Kaolinite RP2 fabric map. Mixed symbols represent changes in observed particle association mode due to boundary conditions.

Finally, the fabric map developed for the particular kaolinite clay tested in this study taking into consideration sedimentation, viscosity and liquid-limit tests (different solids content and strain conditions) closely resembles the fabric map proposed in Figure 2 on the basis of physical processes and scattered data found in the literature.

#### ACKNOWLEDGMENTS

Support for this research was provided by the National Science Foundation, the Georgia Mining Association and The Goizueta Foundation.

#### REFERENCES

- Anandarajah, A. (1997) Structure of sediments of kaolinite. *Engineering Geology*, **47**, 313–323.
- Barak, P. and Nater, E.A. (2003) The virtual museum of minerals and molecules 1998–2003. [http://www.soils.wisc.edu/virtual\\_museum/](http://www.soils.wisc.edu/virtual_museum/) and [http://www.soils.umn.edu/virtual\\_museum/](http://www.soils.umn.edu/virtual_museum/) (modified 09 July 2003; accessed 22 October 2003). University of Wisconsin-Madison.
- Bohn, H.L., McNeal, B.L. and O'Connor, G.A. (1985) *Soil Chemistry*, 2<sup>nd</sup> edition. John Wiley & Sons, New York, 341 pp.
- Brady, P.V. and Walther, J.V. (1989) Controls on silicate dissolution rates in neutral and basic pH solutions at 25°C. *Geochimica et Cosmochimica Acta*, **53**, 2823–2830.
- British Standard (BS) 1377-90 Section 4 (1990) Determination of Liquid Limit.
- Chen, J. and Anandarajah, A. (1998) Influence of pore fluid composition on volume of sediments in kaolinite suspensions. *Clays and Clay Minerals*, **46**, 145–152.
- Di Maio, C. (1996) Exposure of bentonite to salt solution. *Geotechnique*, **46**, 695–707.
- Fam, M. and Dusseault, M. (1998) Evaluation of surface-related phenomena using sedimentation tests. *Geotechnical Testing Journal*, **21**, 180–184.
- Hiemenz, P.C. (1986) *Principles of Colloid and Surface Chemistry*, 2<sup>nd</sup> edition. Marcel Dekker, Inc., New York, 815 pp.
- Hunter, R.J. (2001) *Foundations of Colloid Science*, 2<sup>nd</sup> edition. Oxford University Press, New York, 806 pp.
- Imai, G. (1980) Settling behavior of clay suspension. *Soils and Foundations*, **20**, 61–77.
- Israelachvili, J. (1992) *Intermolecular and Surface Forces*, 2<sup>nd</sup> edition. Academic Press, London, 450 pp.
- Klein, K. (1999) Electromagnetic properties of high specific surface minerals. PhD thesis, Georgia Institute of Technology, Atlanta, Georgia, USA, 335 pp.
- Lambe, T.W. and Whitman, R.V. (1969) *Soil Mechanics*. John Wiley & Sons, New York, 553 pp.
- Lyklema, J. (1995) *Fundamentals of Interface and Colloid Science Volume II: Solid-Liquid Interfaces*. Academic Press, New York.
- Melton, I.E. and Rand, B. (1977) Particle interactions in aqueous kaolinite suspensions III. Sedimentation volumes. *Journal of Colloid and Interface Science*, **60**, 331–336.
- Michaels, A.S. and Bolger, J.C. (1962) Settling rates and sediment volumes of flocculated kaolin suspensions. *Industrial and Engineering Chemistry Fundamentals*, **1**, 24–33.
- Michaels, A.S. and Bolger, J.C. (1964) Particle interactions in aqueous kaolinite dispersions. *Industrial and Engineering Chemistry Fundamentals*, **3**, 14–20.
- Mitchell, J.K. (1993) *Fundamentals of Soil Behavior*. John Wiley & Sons, New York, 437 pp.
- Nicol, S.K. and Hunter, R.J. (1970) Some rheological and electrokinetic properties of kaolinite suspensions. *Australian Journal of Chemistry*, **23**, 2177–2186.
- O'Brien, N.R. (1971) Fabric of kaolinite and illite floccules. *Clays and Clay Minerals*, **19**, 353–359.
- Patton, T.C. (1979) *Paint Flow and Pigment Dispersion*, 2<sup>nd</sup> edition. John Wiley & Sons, New York, 631 pp.
- Pierre, A.C. and Ma, K. (1999) DLVO theory and clay aggregate architectures formed with AlCl<sub>3</sub>. *Journal of the European Ceramic Society*, **19**, 1615–1622.
- Pierre, A.C., Ma, K. and Barker, C. (1995) Structure of kaolinite flocs formed in an aqueous medium. *Journal of Materials Science*, **30**, 2176–2181.
- Rand, B. and Melton, I.E. (1977) Particle interactions in aqueous kaolinite suspensions I. Effect of pH and electrolyte upon the mode of particle interaction in homoionic sodium kaolinite suspensions. *Journal of Colloid and Interface Science*, **60**, 308–320.
- Rand, B., Pekenc, E., Goodwin, J.W. and Smith, R.W. (1980) Investigation into the existence of edge-face coagulated structures in Na-montmorillonite suspensions. *Journal of the Chemical Society, Faraday Transactions I*, **76**, 225–235.
- Ravisangar, V. (2001) The role of sediment chemistry in stability and resuspension characteristics of cohesive sediments. PhD thesis, Georgia Institute of Technology, Atlanta, Georgia, USA, 297 pp.
- Santamarina, J.C., Klein, K.A., Palomino, A. and Guimaraes, M.S. (2002) Micro-scale aspects of chemical-mechanical coupling – interparticle forces and fabric. Pp. 47–64 in: *Chemical Behaviour: Chemo-Mechanical Coupling from Nano-Structure to Engineering Applications* (C. Di Maio, T. Hueckel, and B. Loret, editors). Maratea, Balkema, Rotterdam, The Netherlands.
- Schofield, R.K. and Samson, H.R. (1954) Flocculation of kaolinite due to the attraction of oppositely charged crystal faces. *Faraday Society Discussions*, **18**, 135–145.
- Secor, R.B. and Radke, C.J. (1985) Spillover of the diffuse double layer on montmorillonite particles. *Journal of Colloid and Interface Science*, **103**, 237–244.
- Sridharan, A. and Prakash, K. (1999) Influence of clay mineralogy and pore-medium chemistry on clay sediment formation. *Canadian Geotechnical Journal*, **36**, 961–966.
- Stumm, W. (1992) *Chemistry of the Solid-Water Interface*. John Wiley & Sons, New York, 428 pp.
- van Olphen, H. (1977) *An Introduction to Clay Colloid Chemistry*, 2<sup>nd</sup> edition. Krieger Publishing Company, Malabar, Florida, USA, 318 pp.
- Wieland, E. and Stumm, W. (1992) Dissolution kinetics of kaolinite in acidic solutions at 25°C. *Geochimica et Cosmochimica Acta*, **56**, 3339–3355.
- Wroth, C.P. and Wood, D.M. (1978) The correlation of index properties with some basic engineering properties of soils. *Canadian Geotechnical Journal*, **15**, 137–145.

(Received 28 May 2004; revised 5 January 2005; Ms. 919)